

Modeling and experimental validation of a dynamic regional saturation J-A model for protective current transformer

Duan Jiandong^a, Li Hao^{a,*}, Lei Yang^b

^a Department of Electrical Engineering, Xi'an University of Technology, Xi'an, Shaanxi 710048, China

^b Xi'an Thermal Power Research Institute Co., Ltd., Xi'an 710054, China

ARTICLE INFO

Keywords:

Protective current transformer
Improved J-A model
Dynamic regional saturation
Transient test

ABSTRACT

The analysis and accuracy of modeling the protective current transformer are yet not suitable for a wide range of current levels, especially under weak transient saturation. It is necessary to develop a mathematical tool allowing to create field models of current transformers allow modeling not only steady modes, but also transients ones. With the support of the large current transient test conducted on the real protective current transformers, multiple test levels from 6 to 48 kA transients were obtained. This paper devoted to the study of modeling protective current transformers more accurately proposes an improved dynamic regional saturation J-A model. It emphasizes the excess loss of the core under transient conditions, and designs a numerical solution for the proposed dynamic regional saturation J-A current transformer model without iteration, so that it can simulate the secondary output of the current transformer online. By numerous data which are actually saturated in the transient flow test, the proposed dynamic partitioned saturation J-A model, the static J-A model and the dynamic J-A model are compared and verified, respectively. Extensive results prove the effectiveness of the proposed method, which is capable to modeling protective current transformer transient of the actual situation. And the average error under a wide range test is relatively stable.

1. Introduction

Protective Current Transformer (P CT) has a stake in coordinating relay protection system with safe and reliable operations. However, P CT is easily transiently saturated due to the nonlinear influence of iron core material, which may lead to the failure or misoperation of the relay protection at the secondary side [1]. With the development of technology, the study of CT transient characteristics has gradually changed from linear analysis and physical simulation experiments to digital simulation. The linear equivalence analysis obviously cannot explicate saturation, and the means of extensive physical experiments is very costly [2]. Therefore, it is an urgent and primary task to accurately reproduce the secondary signal in the form of instantaneous values.

Among various models in current transformers [3,4]: The piecewise linear model is suitable for rough discussions due to the omission of hysteresis. The Preisach model is widely accepted but difficult to implement in circuit calculation. The J-A theory has been adopted to simulate the CT model in some professional software, such as PSCAD/EMTDC [5–7], for ease of time-step implementation. However, under a wide range of current levels, the accuracy of the model calculation results is decentralized in practical applications [8,9], and the

saturation characteristics cannot be fully and accurately exhibited for analyzing the effects on protection especially in transient modes. Therefore, the further study on CT modeling is needed [10,11].

In general, the J-A models include static and dynamic ones due to the different applications in frequency domains. The static model, being of the classical J-A theory, only considers hysteresis in magnetization. The dynamic, considering the dynamic energy consumption, is suitable of modeling the hundreds of kilohertz. Being of dynamic J-A model, it is most accepted by the separation magnetic field strength in the form of hysteresis, classical eddy current, and excess loss [12,13]. While the calculation of the excess loss is hard to achieve, dealing with a constant coefficient or the neglect of the excess loss are questionable and accuracy is poor in decay transient situation. The other type is to represent the dynamic model by using differential magnetization of the high-frequency field [14]. There is a difference in the form, but conceptually from the separation dynamic one, the eddy current effect and decay effect in the high-frequency field are also considered. The identification of extra damping factor and natural resonant frequency have been discussed in [15]. Besides, much research works on the application of J-A theory to the improvement of ferromagnetic element modeling [16–18]. Facing to the transient saturation of current transformers,

* Corresponding author.

E-mail addresses: duanjid@xaut.edu.cn (J. Duan), li_hao_xaut@163.com (H. Li).

<https://doi.org/10.1016/j.ijepes.2018.08.029>

Received 25 May 2018; Received in revised form 26 July 2018; Accepted 22 August 2018

Available online 30 August 2018

0142-0615/ © 2018 Elsevier Ltd. All rights reserved.

these methods still lack the work to be verified at a wide-range flow test [19,20] and the accuracy may be poor in some transient situations. This is because the silicon steel plate technology used in CT can reduce the eddy current effect. The more important is the consideration of excess loss in the transient saturation environment. And the actual CT transient saturation phenomenon is difficult to reproduce often in the laboratory, the actual data is rare, the accurate model suitable for CT transient saturation is particularly important.

In this paper, the concept of regional saturation is introduced to improve the dynamic J-A model of current transformers, and the problem of excess loss of cores under transient conditions is emphasized. The numerical solution for the non-iterative scheme of the proposed dynamic regional-saturation J-A current transformer model is given. The method enables it to simulate the secondary output of the CT in real time online. A large flow dynamic simulation tests (with a maximum transient current periodic component value up to 48 kA) were carried out, the proposed model is compared with the static J-A model and the dynamic J-A model to perform on real data.

The organization of this paper is as follows: Section 2 reviews the related background and relevant J-A current transformer models. The proposed dynamic regional-saturation J-A current transformer model and the calculation procedures are provided in detail in Section 3. In Section 4, the experiments and the results are discussed. Finally, Section 5 concludes the paper.

2. Theoretical background

2.1. P CT equivalent circuit

The electromagnetic protective current transformer includes core, winding and load (usually connected to the microprocessor relay protection device), as shown in Fig. 1. The core material is made of silicon steel sheet; the single-turn type primary winding is commonly used for high voltage system above 110 kV; the load is up to the power consumption of the microcomputer protection device, which is low and resistive, generally within 2VA.

The CT saturation is magnetic saturation in the core. It has important relationship with the material, geometry, gap and process of the selected core. The magnetization virtually is mapping the relation of $\vec{B} = f(\vec{H})$ or $\vec{H} = f^{-1}(\vec{B})$. The excitation current in the core forms an excitation magnetic field \vec{H} , which in turn generates an induced magnetic field \vec{B} . The changes in the \vec{B} value act directly on the CT transient saturation. Fig. 2 is a \vec{B} - \vec{H} cloud map under a sinusoidal magnetization field. The results show that the current transformer has almost zero angle between \vec{B} and \vec{H} in the core, and the modeling could be simplified into the scalar field one.

The magnetic field models of the core should be connected to the external electrical system. The equivalent circuit of a typical P CT is

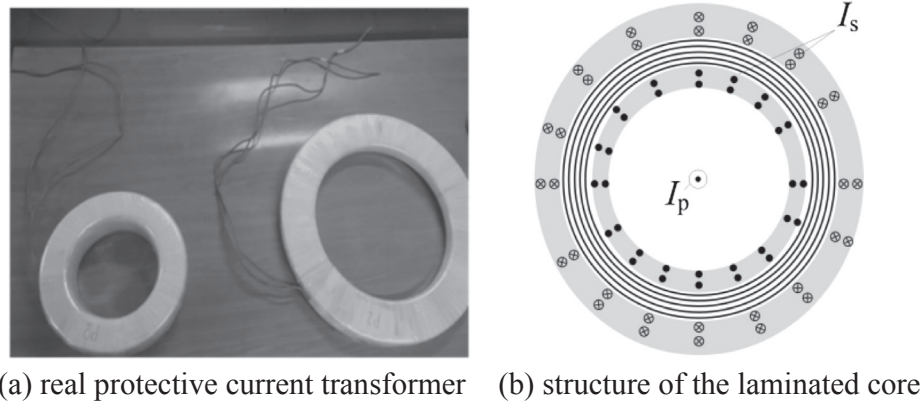


Fig. 1. Protective current transformer and its core structure.

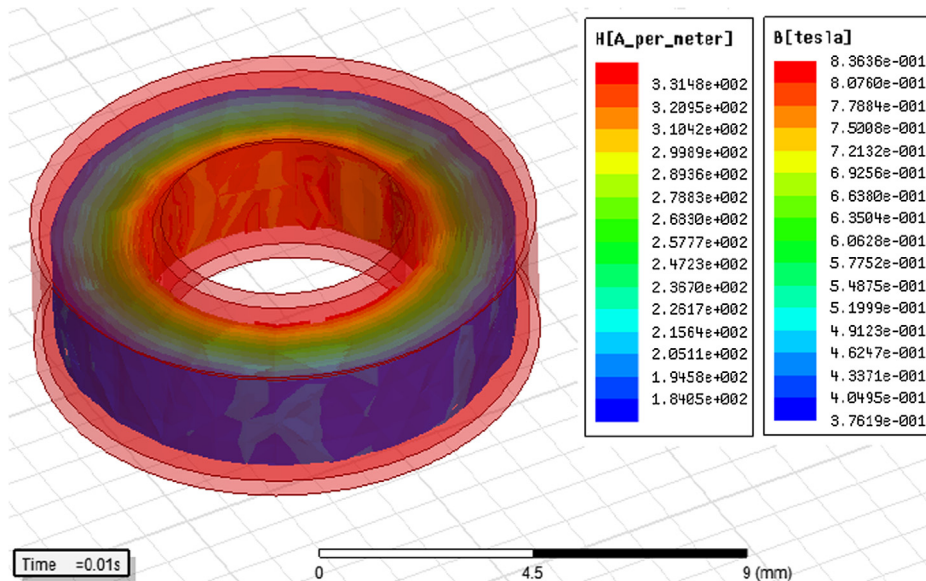


Fig. 2. \vec{B} - \vec{H} distribution under the sinusoidal magnetization field.

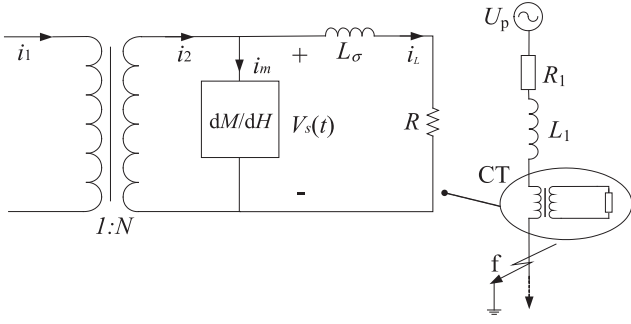


Fig. 3. Equivalent circuit for modeling.

shown in Fig. 3, which consists of an ideal transformer, the dM/dH describing the core excitation and the secondary circuit. The circuit satisfies the following equations:

$$i_2(t) = i_1(t)/N \quad (1)$$

$$i_2(t) = i_m(t) + i_L(t) \quad (2)$$

$$v_2(t) = i_L(t) \cdot R + L_\sigma \cdot di_L(t)/dt \quad (3)$$

According to formula (4) and (5), the relationship between the excitation current in the circuit and the magnetic field of the core are linked together, and excitation current can be deduced as Eq. (6).

$$v_2(t) = N \frac{d\phi}{dt} = \mu_0 N A \frac{d(H + M)}{dt} \quad (4)$$

$$H = \frac{N \cdot i_m}{l} \quad (5)$$

$$\frac{di_m}{dt} = \frac{l \cdot (R \times (i_2 - i_m) + L_\sigma \cdot di_2/dt)}{\mu_0 N^2 A (1 + dM/dH + L_\sigma)} \quad (6)$$

where L_σ is the leakage inductance of windings; R is the load on secondary side (including the winding loss); A is the equivalent core cross-sectional area; N is the CT secondary winding turns.

Then the current transformer can be modeled precisely after matching the accurate hysteresis properties of the core, which refers to the solution of dM/dH .

2.2. Static J-A model

The so-called static J-A is the classic J-A model. The basic idea is that the magnetization M is divided hypothetically into two parts: the reversible component and the irreversible component. The classical J-A model uses the Langevin equation (7) to describe the $M_{an}-H_e$ relationship.

$$M_{an} = M_s \left(\coth \left(\frac{H_e}{a} - \frac{a}{H_e} \right) \right) \quad (7)$$

where M_s is the saturation magnetization of the core material, a is the domain wall coupling coefficient, a is the shape parameter, H_e is the effective magnetic field strength, and the relationship with the actual magnetic field is described as Eq. (8),

$$H_e = H + \alpha \cdot M \quad (8)$$

Finally, M_{an} together with the reversible and the irreversible magnetization, the dM/dH deduced by the static J-A theory is shown as Eq. (9).

$$\frac{dM}{dH} = \frac{\delta \cdot (1 + c)(M_{an} - M)}{k \cdot \text{sign}(\dot{H})(1 + c) - \alpha(M_{an} - M)} + c \cdot \frac{dM_{an}}{dH} \quad (9)$$

where the δ and $\text{sign}(\cdot)$ are given by

$$\delta = \begin{cases} 0 & \text{sign}(\dot{H}) \times (M_{an} - M) \leq 0 \\ 1 & \text{else} \end{cases} \quad (10)$$

$$\text{sign}(\dot{H}) = \begin{cases} 1, & dH/dt > 0 \\ -1, & dH/dt < 0 \end{cases} \quad (11)$$

For a given P CT and the known J-A parameters, the magnetic field could be determined and the excitation current i_m can be calculated by solving Eq. (6) using MATLAB. Then the calculation of the secondary current can be obtained by Eq. (2).

2.3. Dynamic J-A model

The dynamic model is proposed mainly to consider the dynamic characteristics of the eddy current. There are always excess-loss between the power-frequency measured and the modeled magnetization [12], which has little effect on the hysteresis modeling of air gap electromagnetic devices such as motor. But for electromagnetic device for closed magnetic circuits such as transformers and CTs, which is easy to conduct to imprecise results in general case. A dynamic model with energy separation is given by:

$$W_{tot} = W_h + W_{class} + W_{exc} \quad (12)$$

where W_{tot} is the total energy loss in the core, W_h means the hysteresis, W_{class} is the classical eddy effect, and W_{exc} refers to the excess-loss.

Each component of W_{tot} can be represented by the component of magnetic field H for the convenience of calculation, that is, $H_{(t)} = H_h + H_{class} + H_{exc}$. A commonly accepted expression is by:

$$H(t) = H_h(B) + \frac{d}{12\rho} \frac{dB}{dt} + g(B)\mu \left| \frac{dB}{dt} \right|^{0.5} \quad (13)$$

where d is the thickness of the core silicon steel; ρ is the resistivity; $g(B)$ is a function of the magnetic induction intensity; μ is the differential change direction of B , when the increment is positive, μ is set to be 1, or is -1.

It can be seen that in this kind of dynamic magnetic field calculation, the second is linearly related to the differential magnetic density, and the third is nonlinearly related to the square root term of the differential magnetic density. If $g(B)$ is not selected properly, the accuracy will be reduced, or would increase the computational complexity.

There is also a dynamic magnetization model described purely by differential function whose dynamics are reflected in the magnetization correction, as shown in:

$$\frac{d^2 M_f(t)}{dt^2} + 2\lambda \frac{dM_f(t)}{dt} + \omega_n^2 M_f(t) = \omega_n^2 M(H) \quad (14)$$

where λ is the attenuation constant, ω_n is the natural frequency, and M_f is the magnetization value after taking the dynamic loss into account. Adding two parameters, This dynamic J-A model can be calculated and solved [15].

After the considerations about the dynamics, the dM/dH still needs to be calculated. And as the static J-A model the secondary current can be obtained.

3. The proposed method

The representation of the energy separation of the core is bound to have the problem that the excess loss function (coefficient) is hard to be determined. Therefore, in this paper, the dynamic magnetization model is still described in the form of differential equations, that is, the magnetization process mainly solves the real-time dM_f/dH in the equivalent circuit of the CT. The first order differential expression of dM/dt about Eq. (14) is firstly expressed as follows:

$$\begin{cases} \frac{dM_f(t)}{dt} = y \\ y' = \omega_n^2(M(H) - M_f(t)) - 2\lambda y \end{cases} \quad (15)$$

Through the differential equation of analytic (15), it is easy to have that when $\lambda \geq \omega_n$, the differential equation has real solution. The analytic equivalent of the general and special solution of $M_f(t)$ are given by:

$$y = P_m(M(H))e^{(-\lambda \mp \sqrt{\lambda^2 - \omega_n^2})M(H)} \quad (16-a)$$

$$y^* = M(H)^\mu Q_m(M(H))e^{(-\lambda \mp \sqrt{\lambda^2 - \omega_n^2})M(H)} \quad (16-b)$$

μ is related to the order of $P_m(M(H))$ polynomials, that is, $\lambda = \omega_n$, $\mu = 1$; when $\lambda \neq \omega_n$, $\mu = 0$.

The high frequency dynamic described in this solution is comprehensive, but for the modeling the current transformer transients, the signal energy of the high frequency noise in the system is weak. Coupled with the stack process of the CT core, the eddy current within the core is not obvious. Therefore, the reservation form of (15) is simplified to:

$$\frac{d^2 M_f(t)}{dt^2} + \lambda_0 \frac{dM_f(t)}{dt} = C \cdot M(H) \quad (17)$$

In this condition, the solution can be:

$$y = C_1 e^{-\lambda_0 M(H)} + C_2 \quad (18)$$

where C_1 is a variable depending on $dM(H)/dt$, C_2 is a constant, and

$$\lambda_0 = C \left(\frac{2\lambda}{\omega_n^2} + \frac{M_f(t)}{dM/dH \cdot (dH/dt)} \right) \quad (19)$$

If the natural attenuation and corresponding natural frequency is been overlooked and the core magnetic field is in weak saturation region, the average permeability is relatively high. Eq. (20) can be obtained.

$$\lim_{dM/dH \rightarrow \infty} \lambda_0 = 0 \quad (20)$$

It can be concluded that the $\lambda_0 = 0$ is equivalent to $dM_f(t)/dt$ doubling a constant through (18).

When the core is in the heavy saturation region, the average permeability changes slowly. At this time, the permeability and the magnetic field increase slowly, and the equivalent effect is to the $dM_f(t)/dt$ adding a uniform-phased constant of the magnetization change through Eq. (18).

In order to reduce the complexity of solving differential equations, the modified Eq. (17) is implemented by multiplication constant or additive constant, depending on where the saturation condition of the core might be. Among them, the judgement of dM_f/dH belongs to light or heavy saturation should be determined automatic and real-time.

Hence, it is assumed that there is no hysteresis in the magnetization process, that is, the $M-H$ relation satisfies the Langevin equation. The differential expression of the formula (7) in the form of time domain is obtained as:

$$\frac{dM}{dt} = \frac{M_s}{a} \left[1 - \coth^2 \left(\frac{H}{a} \right) + \left(\frac{a}{H} \right)^2 \right] \cdot \frac{N}{l} \cdot \frac{di_m}{dt} \quad (21)$$

which is prone to get $\frac{dM}{dt} \leq \frac{M_s}{a} \cdot \frac{N}{l} \cdot \frac{di_m}{dt}$. According to the concept of reversible magnetization $M_{rev} = c(M_{an} - M)$. This definition is simplified by calculating the magnetic domain energy loss and neglecting the three higher order terms, that is, the reversible magnetization part considering the hysteresis is smaller than the actual one. Therefore, the derivation of its susceptibility form could be given by:

$$\left(\frac{dM_{an}}{dH} - \frac{dM}{dH} \right) \cdot \frac{dH}{dM_{rev}} > \frac{1}{c} \quad (22)$$

If the Langevin equation of the original field H_e is scaled again,

according to Eq. (21), it is easy to get $\frac{dM_{an}}{dt} \leq \frac{M_s}{a} \cdot \frac{dH_e}{dt}$. According to the combination with Eq. (22), it has the following inequality:

$$\frac{M_s}{a} \left(\frac{dH}{dt} - \frac{dH_e}{dt} \right) \cdot \frac{dt}{dM_{rev}} < \frac{1}{c} \quad (23)$$

According to the relation of $H_e = H + \alpha M$, since the α is constant and less than 1, the formula (23) is resized again, and the judgment threshold of the heavy or weak magnetic saturation field can be judged automatically. When formula (24) satisfies, it is judged to be the weak magnetic saturation region, which is calculated according to the simplified dynamic magnetization formula; otherwise, it is heavy magnetic saturation, and need not consider the current dynamic process.

$$\frac{dM}{dt} \leq \frac{N}{ac \cdot l} M_s \quad (24)$$

Thus, in the improved dynamic magnetization J-A model, the dynamic susceptibility is corrected in real time with the saturation of the two regions, and the dM_f/dH at this time is calculated for calculation of the excitation current of the current transformer core, as shown in Eq. (25). The known primary current input can be used to calculate the differential equation of the current excitation current to restore the secondary current of the CT, finally.

$$\frac{di_m}{dt} = \frac{l \cdot (R_2 \times (i_l/N - i_m) + L_2 \cdot di_l/dt/N)}{\mu_0 N^2 A (1 + dM_f/dH + L_2)} \quad (25)$$

In the current work on the improvement of the dynamic regional saturation of the J-A theory, there is no influence on the concept of original two components of the magnetization part (reversible magnetization, irreversible magnetization), only the description of the original stationary state is changed into a differential form, and the expressions of the calculation are given by (26):

$$\frac{dM_{irr}}{dH} = \frac{M_{an}(H_e) - M_{irr}}{k \cdot \text{sign}(\dot{H}) - \alpha [M_{an}(H_e) - M_{irr}]} \quad (26-a)$$

$$\frac{dM_{rev}}{dH} = c \left(\frac{dM_{an}}{dH} - \frac{dM_f}{dH} \right) \quad (26-b)$$

The algorithm for the CT secondary calculation consists of the following steps, and the detailed calculation of the algorithm is depicted in Fig. 4.

(1) Initialization of electromagnetic calculation

In order to improve the efficiency of the algorithm calculation and easy to integrate with PSCAD/EMTDC, MATLAB and other software, this paper selects a fixed-step numerical calculation mode without iterative cycle. In the initialization, it is necessary to obtain: CT model parameters, core size, and secondary load. Meanwhile, simulation parameters need to be set, including offline identified J-A model parameters, calculation steps, and $i_m(i-1)$ and $M(i-1)$ recorded at the previous moment (the initial $i_m(i-1)$ cannot be 0 and must be set to a small value if necessary).

(2) Update the relationship of $M(H)$

$M(H)$ is the portion of the magnetization in $M_f(t)$ that only accounts for the hysteresis loss and is also the most important part of the M_f . First, update the current magnetic field strength $H(i)$ with the historical excitation current $i_m(i-1)$, consider the Weiss coupling, update $H_e(i)$ with $M(i-1)$, and obtain $dM_{an}/dH(i)$ using the Langevin differential expression, then into Eq. (9), to obtain the preliminary $M(H)$ relationship.

(3) Regional saturation judgment and update $dM_f(t)/dH$

In order to enhance the efficiency of online real-time calculation,

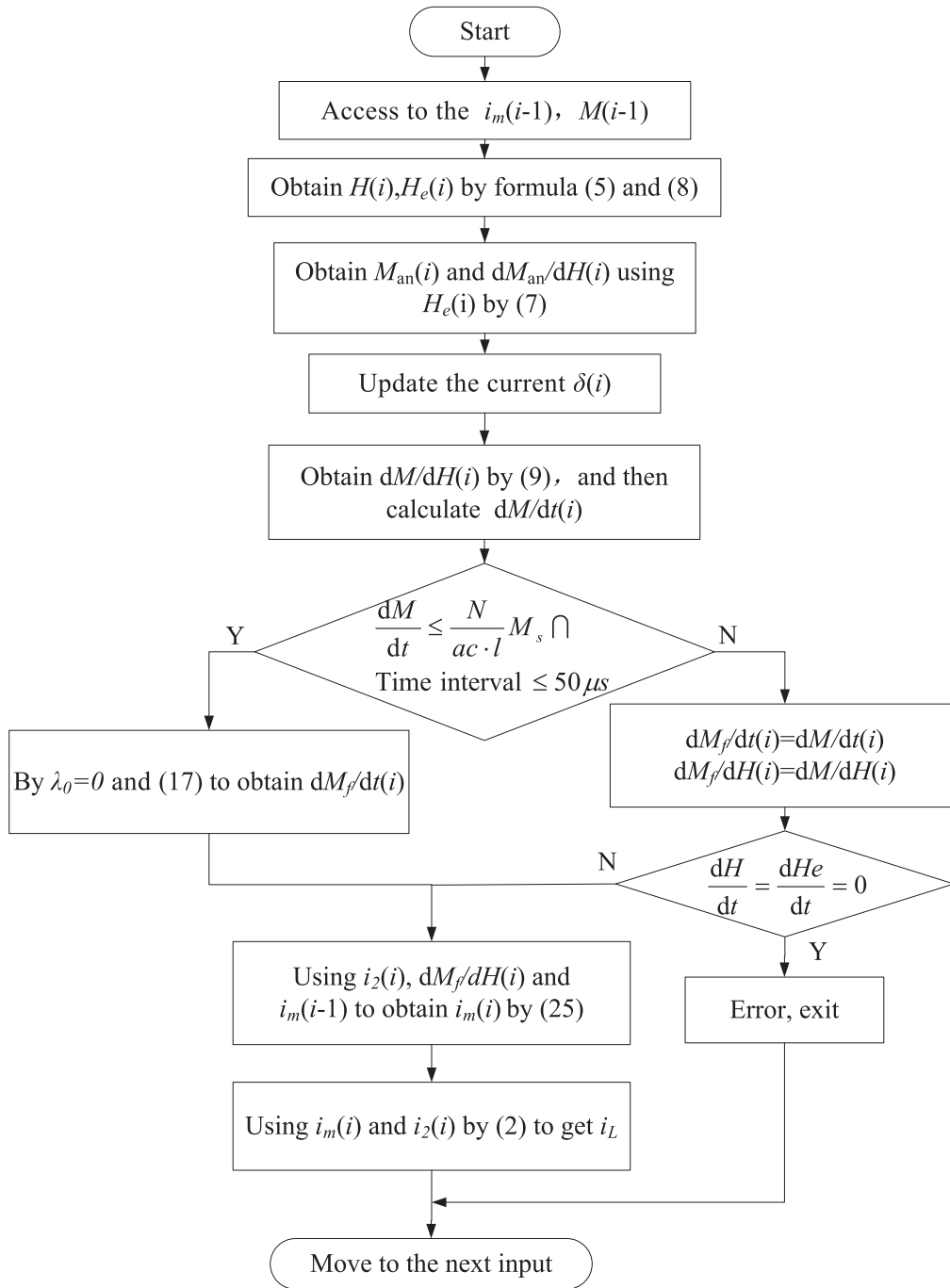


Fig. 4. Flow chart of dynamic partitioned saturation J-A model.

this paper only considers the two-segment regional saturation classification. The simplification in the selection of regional judgments is also slightly rough; making the macro-magnetic conductivity is slightly lower in the heavy saturation region, so it is necessary to use a high time resolution calculation interval to avoid the instability of the result caused by the difference instead of the differential. In this paper, the recommended calculation step length could be 50 us/point. For the PSCAD/EMTDC test, the sampling with or within this step could satisfy the simulation of the 330 kV power system short-circuit transient readily.

In order to avoid non-data results in the calculation, dH/dt and dH_e/dt are used as condition monitoring values. Once the value of 0 is detected, the calculation is immediately jumped out and an error is reported.

(4) Update the excitation condition to solve the CT secondary current

The excitation current micro-increment di_m/dt is calculated by Eq. (25), and the current $i_m(i)$ is updated with the historical magnetization current $i_m(i-1)$. Thus, the secondary current $i_2(i)$ can be calculated using the given primary-side current value $\{i_1(i-1)/N, i_1(i)/N\}$. Then record the current $M_f(i)$ and $i_m(i)$ as the next calculated initial value: $M(i-1)$ and $i_m(i-1)$.

(5) Calculation exit

According to the above steps, it is repeatedly updated. When the calculation time meets the setting and there is no error alarm, the calculation cycle of the numerical model is terminated, and the CT

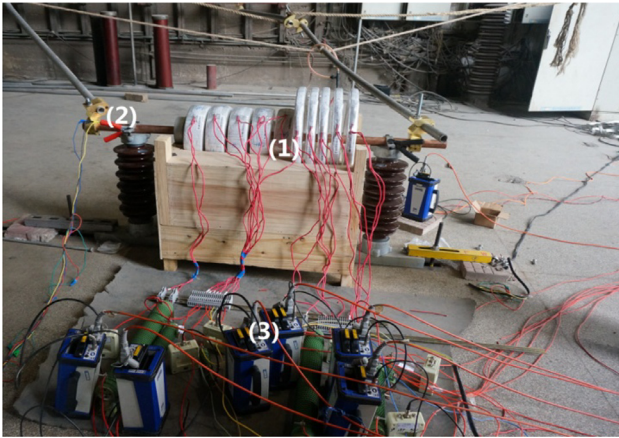


Fig. 5. Test site wiring: (1) protective current transformers, (2) primary bus (3) recording devices on the secondary side.

secondary currents are the main output.

As already mentioned, the J-A dynamic regional saturation model of the current transformer established in this paper is improved on the basis of the dynamic J-A model. It not only considers the saturation loss of the core hysteresis, but also considers the magnetization process under the saturation of the dynamic region for the characteristics of transient saturation. And the numerical calculation of the fixed step could realize the online real-time simulation of CT transient saturation model, and it is easy to nest or co-simulate with professional software.

4. Experiments and discussions

4.1. Large current dynamic test

Based on the earlier analysis [9], this paper has studied and carried out the large current dynamic transient test on the real protective current transformer. In this experiment, a series of current transformer coils of different loads are tested in series, and the test scene is shown in Fig. 5.

This paper selects the maximum short-circuit current under a 330 kV system at a certain region power flow control section in China as the maximum test current bound, which is up to 48 kA. According to the actual operating conditions of the CT, design the transient flow test; superimpose the non-periodic component of the attenuation to simulate the short-circuit fault current; control the reclosing timing to obtain the maximum remanence; use the actual cable, protection and fault recording device as the load conditions; multiple sampling and simultaneous sampling of CT primary and secondary currents are performed

using the data acquisition systems, protection and fault recorders. The maximum frequency of data acquisition is 1 MHz. The test conditions carried out are shown in Table 1.

4.2. Results and discussions

Choosing the ratio of 1200/1P CT, with the core size about are: Inside Diameter \times Outside Diameter \times Cross-Sectional Area = 34.5 cm \times 49.5 cm \times (7.5 \times 2.5)cm², the measured $L_\sigma = 0.398$ mH, $R_\sigma = 3.72$ Ω , as the objects to verify the effectiveness of the proposed model. At the same time, the static J-A and dynamic J-A are also introduced into the experimental calculation and analysis. The static J-A uses the classical Langevin describing M_{an} model; the dynamic J-A selects the model in [10] as a comparison, in which all the model parameters of the J-A theory are all from the same set shown as Table 2.

Figs. 6 and 7 show the calculated waveforms of the P CT with 4 Ω at the transient current levels of 6 kA and 30 Ω load at 48 kA, respectively. In the case of light saturation as shown in Fig. 6, the difference among three models is obvious. From the partial observation, the improved model is shown being able to catch the actual fault phase amplitude information better than the static and the dynamic models. In the heavy saturation operation as Fig. 7, the waveforms of the three models are all close to the actual test data. It can be seen from the partial chart of the first cycle that the coincidence degree between the static model and the improved model and the experimental data is better than that of the dynamic model.

The results of more group tests were evaluated by means of two indexes, mean square deviation IRMS and similarity R_r .

$$IRMS = \sqrt{\frac{1}{N} \sum (I_{test} - I_{model})^2} \quad (24)$$

$$R_r = \frac{N \sum I_{test} I_{model} - \sum I_{test} \sum I_{model}}{\sqrt{[N \sum I_{test}^2 (\sum I_{test})^2] [N \sum I_{model}^2 (\sum I_{model})^2]}} \quad (25)$$

where N is the total number of selected data; I_{test} is the secondary side current waveform from test; I_{model} is the secondary side current waveform from the model calculation.

Fig. 8 is a comparative evaluation of index R_r . The regional characteristics of the three models are easy to be observed. When the load is light, the current level is not high and the saturation of the core is weak, the static J-A model cannot describe such transient circumstance well, and the error is slightly larger. The dynamic loss of dynamic model is considered to help improve the accuracy, but the effect of the dynamic model under the heavy saturation zone appears to be overfed. The improved dynamic regional saturation model has good calculation results in all transient saturated working regions, and the average calculation accuracy is shown to be higher than other two models.

Table 1

Transient test conditions.

Test number	Short circuit period component (kA)	Load (Ω)	Non-periodic components		Remanence (%)	Reclosing time (s)
			Initial value (%)	Attenuation constant (s)		
1	6	4.34	95%	0.1	0	0.684
2	6	7.85	95%	0.1	0	0.684
3	6	29.28	95%	0.1	0	0.684
4	12	4.34	100%	0.1	0	0.671
5	12	7.85	100%	0.1	4%	0.671
2	12	29.28	100%	0.1	0	0.671
7	24	4.34	89%	0.1	0	0.684
8	24	7.85	89%	0.1	2%	0.684
9	24	29.28	89%	0.1	−2%	0.684
10	48	4.34	80%	0.1	5%	0.678
11	48	7.85	80%	0.1	−10%	0.678
12	48	29.28	80%	0.1	0	0.678

Table 2
Parameters of the CT J-A model.

a	α	c	k	M_s
100	2.5×10^{-5}	0.1	500	1.7×10^6

The calculation results of three models in transient 6kA, 12kA, 24kA, 48kA and three load levels are evaluated and calculated in turn, which are all from the large current test. The comparison of the results is shown in Table 3.

According to the detailed results of Table 3, when the load is close to the actual protective device, the improved model has a mean current variance of 0.72A in the transmission 5A transient current(6kA converted to the secondary side); the IRMS of the transfer 10A transient current (12kA converted to the secondary side) is 0.97A; the 20A transient current (24kA converted to the secondary side) IRMS is 1.71A; the highest transient 40A (48kA converted to the secondary side) IRMS is 1.76A, which is 30% smaller than the static model, and 5.9% smaller than that of the dynamic model. The improved model weakens the dynamic loss problem focusing on the high-frequency field, and the hysteresis energy loss correction is performed for the transient

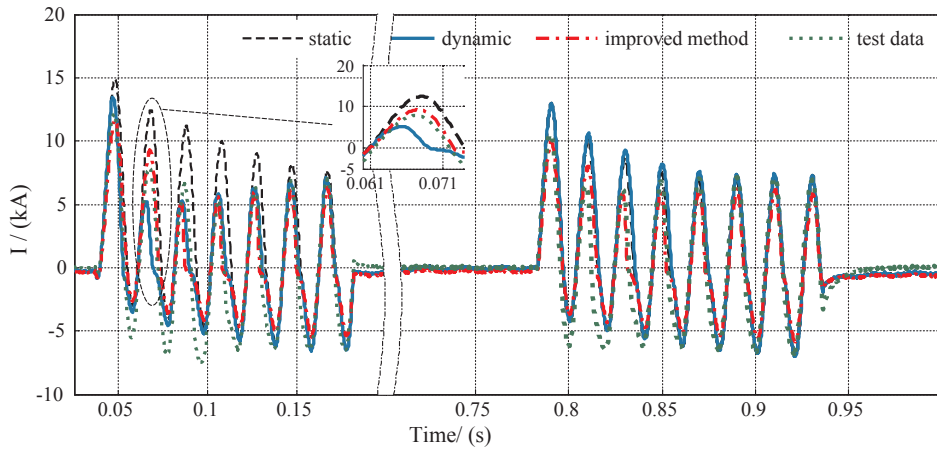


Fig. 6. The results analysis of models under transient 6kA, 4 Ω test.

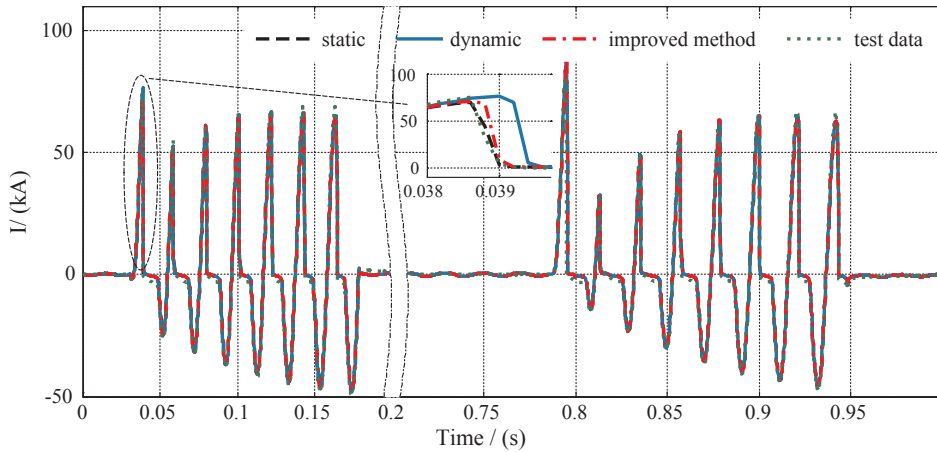


Fig. 7. The results analysis of models under transient 48kA, 30 Ω test.

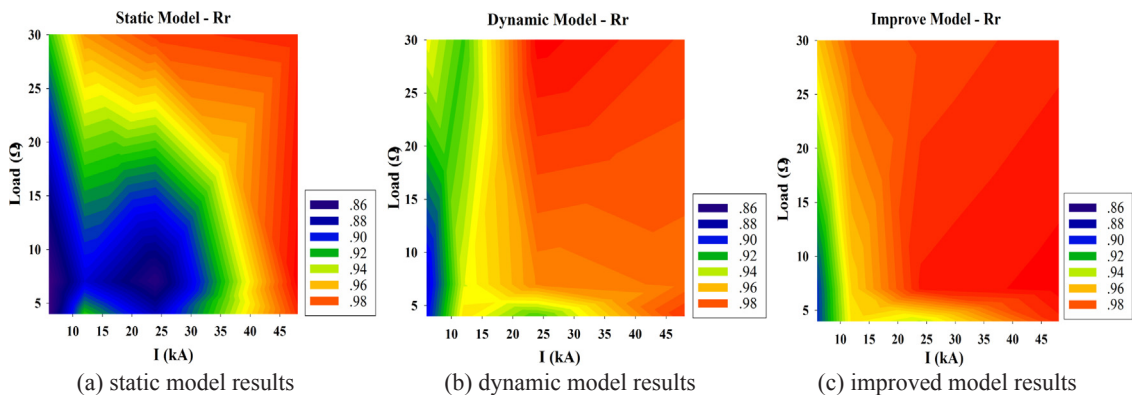


Fig. 8. Evaluation of the effect of the model under R_r .

Table 3
Analytical results for current transformer model.

Transient flow (kA)	Load (Ω)	IRMS (A)			R_r		
		Static J-A	Dynamic J-A	Improved J-A	Static J-A	Dynamic J-A	Improved J-A
6	4	0.9214	0.7665	0.719	0.8489	0.8960	0.9006
	7	0.8583	0.7262	0.6931	0.8461	0.8905	0.9014
	30	0.8331	0.7363	0.4327	0.9230	0.9460	0.9551
12	4	0.9722	0.9024	0.9712	0.9222	0.9504	0.9493
	7	1.7042	0.8593	0.8004	0.8877	0.9434	0.9525
	30	0.6351	0.8044	0.5205	0.9644	0.9267	0.9770
24	4	2.3201	1.9086	1.7104	0.8813	0.9279	0.9392
	7	1.6230	0.9247	0.6397	0.8557	0.9686	0.9888
	30	0.6658	0.6505	0.8148	0.9817	0.9940	0.9807
48	4	2.5262	1.8666	1.7566	0.9853	0.9844	0.9862
	7	1.2044	2.4005	1.2067	0.994	0.9732	0.9939
	30	1.4664	1.6698	1.4886	0.9873	0.9832	0.9866

The bold means the minimum error or the maximum correlation among models.

saturation changing process in the weak magnetic field. Compared with the static and the dynamic model, the accuracy of the improved model is obviously better in the light saturated working area under the flow of 6 ~ 12kA, and a few less than the dynamic model are also close. In the case of deep saturation above 48kA, the static model presents a better reduction effect, and the improved model could also reflect the actual situation.

The dynamic regional saturation model proposed in this paper achieves good results in reducing the wide range transient flow test data. In addition, the numerical calculation of the models in the test is to solve the original data directly under the sampling rate of 50 kHz. The numerical calculation method can adapt to the experimental noise of all data sets, and the model calculation method is also stable.

5. Conclusions

This paper proposes a dynamic regional saturation model for protective current transformers based on dynamic J-A theory. The model ignores the high-frequency eddy current losses that were used and emphasized in conventional dynamic J-A models, and the attention has been paid to the excess loss of the current transformer core in low-frequency electromagnetic transients. The J-A theory is supplemented to improve the differential form of susceptibility correction. Finally, a large number of experimental data verify that the proposed model has advantages over the other two discussed methods. Since the equivalent calculation of the magnetic linkage and flux integral field, which may lead to inaccuracy of the calculation, in the future research work, we will consider in combination with finite element calculations to numerically solve the entire magnetic field of the CT core.

Acknowledgments

This research was supported by the National Key R&D Program of China, with Project No. 2016YFB0900600, the National Natural Science Foundation of China, with Project No. 51877174, the State Key Laboratory of Advanced Electromagnetic Engineering and Technology (Huazhong University of Science and Technology), with Project No. 2018KF001, and the State Key Laboratory of Electrical Insulation and Power Equipment (Xi'an Jiaotong University), with Project No. EIPE18201. Besides, The formulation of the test and the measurement of the data in this article were completed with the support of the staff of Shaanxi Electric Power Research Institute and the Xi'an High voltage Apparatus Research Institute in China. Thanks a lot for their works.

Appendix A. Supplementary material

Supplementary data associated with this article can be found, in the online version, at <https://doi.org/10.1016/j.ijepes.2018.08.029>.

References

- [1] Hunt Rich. Impact of CT errors on protective relays—case studies and analyses. *IEEE Trans Ind Appl* 2012;48(1):52–61.
- [2] Zhang XQ, Zhang YY, et al. Research on saturation test under high current for current transformers. *Power Syst Clean Energy* 2016;32(7):58–64. [in Chinese].
- [3] Narampanawe Nishshanka, et al. Analysis of ultra-thin and flexible current transformer based on J-A hysteresis model. *IEEE Sens J* 2017;17(13):4029–36.
- [4] Fallahnejad M, Afrakhte H. The comparison of two approaches Jiles-Atherton and Preisach in simulating hysteresis cycle. In: *International Conference on Knowledge-Based Engineering and Innovation*, IEEE; 2015. p. 710–13.
- [5] Jiles DC, Atherton DL. Theory of ferromagnetic hysteresis (invited). *J Appl Phys* 1984;55(6):2115–20.
- [6] Jiles DC, Tholke JB, Devine MK. Numerical determination of hysteresis parameters for the modeling of magnetic properties using the theory of ferromagnetic hysteresis. *IEEE Trans Magn* 1992;28(1):27–35.
- [7] Annakkage UD, McLaren PG, Dirks E, et al. A current transformer model based on the Jiles-Atherton theory of ferromagnetic hysteresis. *IEEE Trans Power Del* 2000;15(1):57–61.
- [8] Wei Li, Koh CS. Investigation of the Vector Jiles-Atherton model and the fixed point method combined technique for time-periodic magnetic problems. *IEEE Trans Magn* 2015;51(4):1–6.
- [9] Yang Lei, Jiandong Duan, Xiaoqing Zhang, et al. Identification of current transformer J-A model parameters with large current dynamic simulation experiments. In: *Proceedings of the CSEE*, S1; 2016. p. 240–5 [in Chinese].
- [10] Lebedev Vladimir, et al. Modeling of measuring current and voltage transformers in dynamic modes. In: *International conference on mechanical engineering, automation and control systems*, IEEE; 2014. p. 1–7.
- [11] Carrander Claes, Mousavi SA, Engdahl G. An application of the time-step topological model for three-phase transformer no-load current calculation considering hysteresis. *J Magn Magn Mater* 2017;423:241–4.
- [12] Zirka Sergey E, et al. Static and dynamic hysteresis models for studying transformer transients. *IEEE Trans Power Delivery* 2011;26(4):2352–62.
- [13] Hamimid M, Feliachi M, Mimoune SM. Modified Jiles-Atherton model and parameters identification using false position method. *Phys B Condens Matter* 2010;405(8):1947–50.
- [14] Jiles DC. Frequency dependence of hysteresis curves in non-conducting magnetic materials. *IEEE Trans Magn* 1993;29(6):3490–2.
- [15] Zhang Da Ming, Liu YT, Huang S. Differential evolution based parameter identification of static and dynamic J-A models and its application to inrush current study in power converters. *IEEE Trans Magn* 2012;48(11):3482–5.
- [16] Zou Mi, et al. Improved low-frequency transformer model based on Jiles-Atherton hysteresis theory. *IET Gener Transm Distrib* 2017;11(4):915–23.
- [17] Wang Yang, Liu Z, Chen H. Research on residual flux prediction of the transformer. *IEEE Trans Magn* 2017;53(6):1–4.
- [18] Moradi Arash, Madani S. New technique for inrush current modelling of power transformers based on core saturation analysis. *IET Gener Transm Distrib* 2018;12(10):2317–2324.
- [19] Li Yang, Zhu L, Zhu J. Core loss calculation based on finite-element method with Jiles-Atherton dynamic hysteresis model. *IEEE Trans Magn* 2018;54(3):1–5.
- [20] Aboura Faouzi, Touhami O. Integration of the hysteresis in models of asymmetric three-phase transformer: finite-element and dynamic electromagnetic models. *IET Electr Power Appl* 2016;10(7):614–22.